ORGANOMETALLICS

Article

pubs.acs.org/Organometallics

Influence of the Torsion Angle in 3,3′-Dimethyl-2,2′-bipyridine on the Intermediate Valence of Yb in $(C_5Me_5)_2Yb(3,3'\text{-}Me_2\text{-}bipy)$

Grégory Nocton,*[,†,‡] Corwin H. Booth,[§] Laurent Maron,[∥] and Richard A. Andersen*[,‡,∥]

[†]Laboratoire Hétéroéléments et Coordination, CNRS, Ecole Polytechnique, Route de Saclay, 91128 Palaiseau, France

[‡]Department of Chemistry, University of California—Berkeley, Berkeley, California 94720, United States

[§]Chemical Science Division, Lawrence Berkeley National Laboratory, Berkeley, California 94720, United States

[∥]LPCNO, UMR 5215, Université de Toulouse-CNRS, INSA, UPS, Toulouse, France

Supporting Information

ABSTRACT: The synthesis and X-ray crystal structures of $Cp^*_2Yb(3,3'\text{-}Me_2bipy)$ and $[Cp^*_2Yb(3,3'\text{-}Me_2bipy)]\text{-}[Cp^*_2YbCl_{1.6}I_{0.4}]\cdot CH_2Cl_2$ are described. In both complexes, the NCCN torsion angles are approximately 40°. The temperature-independent value of n_f of 0.17 shows that the valence of ytterbium in the neutral adduct is multiconfigurational, in reasonable agreement with a CASSCF calculation that yields a n_f value of 0.27; that is, the two configurations in the wave function are $f^{13}(\pi^*_1)^1$ and $f^{14}(\pi^*_1)^0$ in a ratio of 0.27:0.73, respectively, and the open-shell singlet lies 0.28 eV below the triplet state (n_f accounts for f-hole occupancy; that is, n_f = 1 when the configuration is f^{13} and n_f = 0 when the configuration is f^{14}). A correlation is outlined between the value of n_f and the individual ytterbocene and bipyridine fragments such that, as the reduction potentials of the ytterbocene cation and the free x,x′-R_2-bipy ligands approach each other, the value of n_f and therefore the f^{13}:f^{14} ratio reaches a maximum; conversely, the ratio is minimized as the disparity increases.

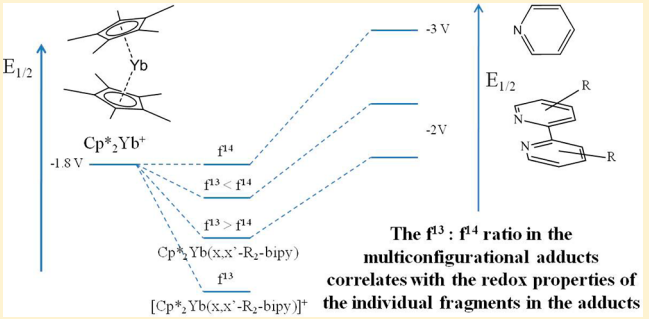

INTRODUCTION

Previous studies of the 2,2′-bipyridine adduct of $(C_5Me_5)_2Yb$, abbreviated $Cp^*_2Yb(bipy)$, have shown that the electronic ground state is multiconfigurational; that is, the f-orbital portion of the ground state wave function includes $\Psi = c_1|Yb(III,f^{13})(bipy^{\bullet-})\rangle + c_2|Yb(II,f^{14})(bipy)^0\rangle$, which is an admixture of two configurations, where c_1 and c_2 are their respective coefficients.[1] The $f^{13}(bipy^{\bullet-})$ configuration is an open-shell singlet, and $f^{14}(bipy)^0$ is a closed-shell singlet; a configuration interaction is therefore possible, since the two configurations have the same symmetry. The outcome of the configuration interaction is that the valence of the ytterbium in $Cp^*_2Yb(bipy)$ is neither +II, where c_1 = 0, nor +III, where c_2 = 0, but is between these two extreme values and therefore intermediate valent. Experimentally, the valence of the ytterbium was obtained from Yb L_{III}-edge XANES spectroscopy and expressed as n_f, the number of f holes: for $Cp^*_2Yb(bipy)$, $n_f = c_1^2 = 0.83(2)$ is temperature independent, and $f^{13}(bipy^{\bullet-})$ is the dominant configuration. The concept that the ground state is multiconfigurational, initially posited by Fulde,[2] was developed from CASSCF calculations, initially using the model $(C_5H_5)_2Yb(bipy)$[1] and then extended to $(C_5Me_5)_2Yb\text{-}(bipy)$ and including four empty bipy orbitals, π^*_1, π^*_2, π^*_3, and π^*_4, in the active space. The calculated value of n_f was 0.86, in agreement with experiment.[3]

When the 2,2′-bipyridine ligand in $Cp^*_2Yb(bipy)$ is replaced by methyl-substituted 2,2′-bipyridine ligands symbolized as x-Mebipy or x,x′-Me_2bipy, where x indicates the position of the methyl group(s) in the 2-pyridyl rings, the ytterbium atom in the resulting adducts is intermediate valent, but the value of n_f is temperature dependent.[3] For example, when x is 5, the value of n_f in $Cp^*_2Yb(5\text{-}Mebipy)$ changes from 0.42 to 0.75 at 300 and 30 K, respectively. The temperature dependence is not due to a closed-shell singlet ⇌ open-shell triplet equilibrium, a valence tautomerism, but to an equilibrium between two open-shell singlet states in which the thermodynamic constants, ΔH and ΔS, are obtained using the Boltzmann equation. The computational model showed that two open-shell singlet states, SS1 and SS2, lie below the triplet by 0.58 and 0.11 eV, respectively.

The evolving model of the electronic structure of the bipyridine adducts of Cp^*_2Yb is (i) the ground state is an open-shell singlet, (ii) the configurations of both fragments, Cp^*_2Yb and the bipyridines, are multiconfigurational, (iii) the number and position of the methyl groups on the bipyridine ligand are significant, and (iv) the n_f values qualitatively track the reduction potential of the free bipyridine ligand, at least for those bipyridines whose reduction potentials are available in the

Received: June 8, 2013

   dx.doi.org/10.1021/om400528d | *Organometallics* XXXX, XXX, XXX–XXX

literature. Item iv provides a strategy for manipulating the value of n_f and therefore the magnetic properties of the adducts. The reduction potential of a ligand is a measure of the HOMO−LUMO energy gap,[1,2] which can be changed by substituents that are electron donors or electron acceptors and by the torsion angle between the 2-pyridyl rings, usually reported as the NCCN angle, obtained from solid-state crystal structures. Electron-donating groups, such as a methyl group, increase the reduction potential relative to hydrogen (Table 1), while a CO_2Me group decreases the potential. Increasing the torsion angle should raise the reduction potential, since twisting the 2-pyridyl groups out of coplanarity will move the energy of π^*_1 closer to the energy of π^*_2 and π^*_3 orbitals. Although the value of the reduction potential for 3,3′-Me_2bipy is not available in the literature, an approximate value is listed in footnote a in Table 1, the energy of the empty orbital should behave qualitatively like those in twisted ethylene.[4] Several examples of methyl- and dimethyl-substituted bipyridine adducts of Cp^*_2Yb have been reported that are consistent with the correlation between n_f and the reduction potential. For this article, we prepared the neutral and cationic adducts between 3,3′-Me_2bipy and Cp^*_2Yb in order to explore the physical properties of the adducts with a bipyridine ligand with a large torsion angle. The results of these and earlier studies support the contention that the redox properties of the individual molecular fragments that comprise the adduct, Cp^*_2Yb and x,x'-Me_2bipy, determine the extent of electron correlation between them.

Table 1. Redox Potential of Selected N-Aromatic Heterocycles and Ytterbocenes

ligand	$E_{1/2}$ (V) vs Fc^+/Fc	ref
py	−3.16	5
4,4′-$(OEt)_2$bipy	−2.88	6
4,4′-Me_2bipy	−2.68	6
bipy[a]	−2.60	7
4,4′-CO_2Me	−2.03	6
$(C_5Me_5)_2Yb^+$	−1.78	8
$(C_5H_4Me)_2Yb^+$	−1.65	9

[a]The approximate value of 3,3′-Me_2bipy lies below −2.8 V (vs Fc^+/Fc, THF/0.1 M $[NBu_4][PF_6]$) but could not be measured precisely under our conditions. Under similar conditions the value of bipy is 2.63 V (vs Fc^+/Fc).

RESULTS

Synthesis and Physical Properties. The preparation of Cp^*_2Yb(3,3′-Me_2bipy) follows the general synthesis procedure used in earlier articles: that is, addition of 3,3′-Me_2bipy to $Cp^*_2Yb(OEt_2)$[10] in toluene followed by crystallization at −20 °C. The green crystals melt at 310−312 °C (Scheme 1).

The cation in $[Cp^*_2Yb(3,3'\text{-}Me_2bipy)][Cp^*_2YbI_2]$ is obtained by addition of the neutral adduct to a suspension of AgI in toluene (Scheme 2). In this case, the identity of the anion depends upon the crystallization solvent.[11,12] If the cation−anion pair is crystallized from warm toluene, the ion pair crystallizes as $[Cp^*_2Yb(3,3'\text{-}Me_2bipy)]$-$[Cp^*_2YbI_2]\cdot{}^1/_3PhMe$. If, on the other hand, the ion pair is crystallized by layering a CH_2Cl_2 solution with pentane, the ion pair has the composition $[Cp^*_2Yb(3,3'\text{-}Me_2bipy)]$-$[Cp^*_2YbCl_{1.5}I_{0.5}]\cdot CH_2Cl_2$, as determined by combustion analysis and integrated intensities in the ^1H NMR spectrum (see the Experimental Section for details). Although the composition of a single crystal is slightly different ($[Cp^*_2Yb$-$(3,3'\text{-}Me_2bipy)][Cp^*_2YbCl_{1.6}I_{0.4}]\cdot CH_2Cl_2$; see below), it is clear that chloride for iodide exchange occurs in dichloromethane, a result not observed in earlier studies of ytterbocene bipyridine cations.[11,12]

X-ray Crystal Structures. ORTEP drawings of the neutral and cationic adducts are shown in Figures 1 and 2, respectively. The crystallographic details are available in the Supporting Information and some bond length and angles are given in Table 2. In both adducts, the coordination number and geometry about ytterbium are the same, as are the torsion angles in the coordinated 3,3′-Me_2bipy ligands, the intramolecular bond angles, and the C(2)−C(2′) distances; the average Yb−N and Yb−C distances, however, are rather different. The average Yb−C distance in the neutral adduct of 2.71 ± 0.01 Å is the same as that found in $Cp^*_2Yb(py)_2$ of 2.74 ± 0.04 Å[13] and in the three independent molecules of Cp^*_2Yb(6,6′-Me_2bipy) of 2.74 ± 0.002 Å.[3] However, the average Yb−N distance of 2.485 ± 0.003 Å is significantly shorter than the equivalent distances in $Cp^*_2Yb(py)_2$ and Cp^*_2Yb(6,6′-Me_2bipy) of 2.565 ± 0.005 and 2.506 ± 0.009 Å, respectively. The average Yb−C distance in the cation of 2.60 ± 0.01 Å is identical with that in $[Cp^*_2Yb(bipy)]^+$ of 2.59 ± 0.01 Å, as are the Yb−N distances of 2.396 ± 0.02 and 2.372 ± 0.005 Å, respectively. The Yb−C and Yb−N distances in the neutral adduct are approximately 0.10 Å longer than in the cation, showing that the valences of Yb are different.

It is noteworthy that the torsion angles of approximately 40°, defined by either the four atoms NCCN and CCCC or the dihedral angle between the planar 3-Me-2-pyridyl rings, are the same in both adducts. The large torsion angle in $[Cp^*_2Yb(3,3'$-$Me_2bipy)]^+$ of 40° and the small angle in $[Cp^*_2Yb(bipy)]^+$ of 7° results in only a slight elongation of the Yb−N distance (0.012 Å) in the former. Hence, the large torsion angle and the resulting "misdirection" of the lone pair of electrons on the bidentate chelate in these cations only slightly lengthens the average Yb−N distances. This, presumably, reflects the small effect on the bond enthalpy difference resulting from the "misdirection". Several crystal structures of 3,3′-Me_2bipy with d transition metals are known, and the twist angle, generally defined as the intersection of the dihedral angle between the planar 3-Me-2-pyridyl rings, ranges from 29 to 37°.[14−20] One exception is $[Ru(Me_3tacn)(3,3'\text{-}Me_2bipy)(OH_2)]^{2+}$, in which the reported twist angle is 54°. However, the structure in the CCDC indicates that the NCCN and CCCC angles are 29 and 43°, respectively.[17]

^1H NMR Studies. The ^1H NMR chemical shifts at 20 °C of the previously prepared bipyridine and substituted bipyridine adducts of Cp^*_2Yb fall into a pattern in which δ(6-H) (∼160 ppm) > δ(4-H) (∼30 ppm) > δ(5-H) (∼10 ppm) > δ(3-H) (∼−15 ppm). The assignments are determined by H for Me group replacement; the approximate values of the chemical shifts are in parentheses.[21] The ^1H NMR spectra show that the

Scheme 1

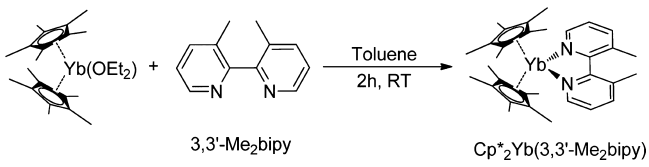

dx.doi.org/10.1021/om400528d | Organometallics XXXX, XXX, XXX−XXX

Scheme 2

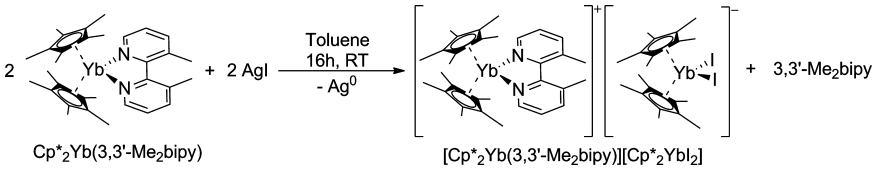

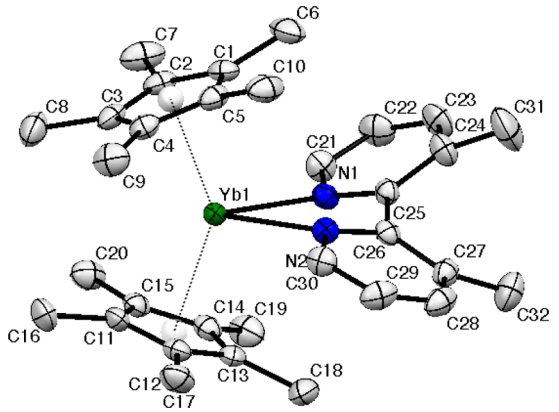

Figure 1. ORTEP drawing of $Cp^*_2Yb(3,3'\text{-}Me_2bipy)$ (thermal ellipsoids at the 50% level). All non-hydrogen atoms have been refined anisotropically, and the hydrogen atoms have been placed in calculated positions but not refined.

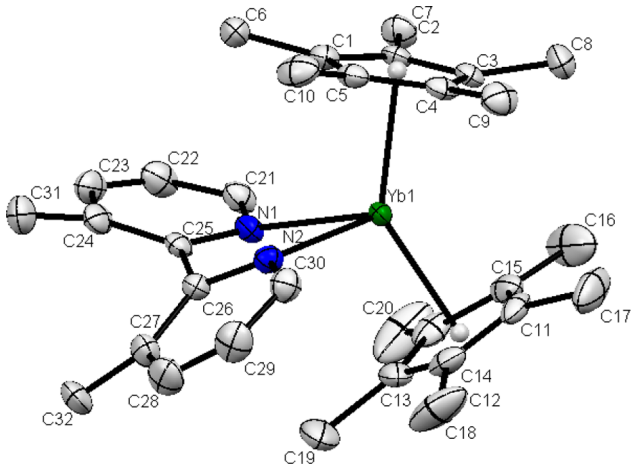

Figure 2. ORTEP drawing of the cation $[Cp^*_2Yb(3,3'\text{-}Me_2bipy)]^+$ (thermal ellipsoids at the 50% level). The anionic partner $[Cp^*_2YbCl_{1.6}I_{0.4}]^-$ and the cocrystallized molecule of CH_2Cl_2 have been removed for clarity. All non-hydrogen atoms have been refined anisotropically, and the hydrogen atoms have been placed in calculated positions but not refined.

adducts have C_{2v} symmetry in solution. The chemical shifts of the 3,3′-Me_2bipy adduct also show four bipy resonances at 20 °C with δ_H values of 32.7, 12.1, 8.5, and 0.58 ppm. The only resonance that can be assigned with certainty is δ_H 0.58, due to the methyl groups in the 3,3′-positions; the δ_H 12.1 resonance is a doublet and therefore is likely due to δ(4-H). The relatively small spread in chemical shift values relative to the large spread in the previously reported adducts of $Cp^*_2Yb(x,x'\text{-bipy})$ where x = H and x′ = Me or x = x′ = Me, implies that the extent of paramagnetism is less in the 3,3′-Me_2bipy adduct. The small range in chemical shift values of the bipy resonances in $Cp_2Yb(bipy)$ of δ_H 53, 18, 11. and 0.6[22] implies that the two adducts have a similar degree of paramagnetism, an inference that is developed below.

A plot of δ vs $1/T$ (Figure 3) of $Cp^*_2Yb(3,3'\text{-}Me_2bipy)$ shows that the most downfield resonance has a strong dependence on temperature and the shift increases with increasing temperature, i.e., the resonance shows anti-Curie behavior. A resonance that follows a Curie Law, $\delta = C/T$, has a positive slope in a δ vs $1/T$ plot, but a slope that is negative displays anti-Curie behavior. This anti-Curie dependence is not due to the exchange between free and coordinated 3,3′-Me_2bipy, since addition of 3,3′-Me_2bipy results in a spectrum at 20 °C due to free and coordinated 3,3′-Me_2bipy resonances. Unfortunately, the inverse temperature dependence of the downfield resonance cannot be interpreted, since the resonance cannot be assigned definitively, although it is most reasonably ascribed to the 6-H position and therefore the value of its chemical shift is dominated by the dipolar contribution to the chemical shift.[12] It is noteworthy that anti-Curie behavior has been shown in low-spin Fe(III) porphyrins to result from a difference in sign between the dipolar and contact shift terms in the chemical shift tensor.[23]

The neutral and cationic adducts of 3,3′-Me_2bipy have C_2 symmetry in the solid state (Figures 1 and 2). The ^{1}H NMR spectrum of the cation in CD_2Cl_2 at 300 K contains four bipyridine resonances at 313, 52, 11, and −18 ppm; the intensity of the last resonance shows that it is due to the methyl groups. Unfortunately, the resonance at δ_H 313 ppm disappears into the baseline as the temperature is lowered and its temperature dependence cannot be determined. In solution, the adducts could have either C_2 or C_{2v} symmetry depending on the value of the torsion angle. In C_{2v} symmetry the average torsion angle is 0° and therefore the methyl groups on each 2-pyridyl ring are eclipsed. Thus, the dynamic process $C_2 \rightleftharpoons C_{2v} \rightleftharpoons C_2$ will have a high activation energy.[24−27] This process cannot be observed in $[Cp^*_2Yb(3,3'\text{-}Me_2bipy)]^{0,+}$, since the two methyl groups are chemically equivalent in either C_2 or C_{2v} symmetry. A way to answer this question would be to prepare adducts in which the C_2 axis is removed: for example, by preparing CpCp′Yb(3,3′-Me_2bipy). Unfortunately, a synthetic methodology for preparing mixed-ring ytterbocences is unknown at the present time.

Visible Spectroscopy. Room-temperature vis−near-IR spectra for $Cp^*_2Yb(3,3'\text{-}Me_2bipy)$ and $[Cp^*_2Yb(3,3'\text{-}Me_2bipy)][Cp^*_2YbCl_{1.5}I_{0.5}]$, recorded in toluene and CH_2Cl_2, respectively, are shown in Figure 4. Two main bands at around 500 nm (20000 cm^{-1}) and 900 nm (11110 cm^{-1}) are present in $Cp^*_2Yb(3,3'\text{-}Me_2bipy)$. These two transitions, attributed to ligand-based $\pi \rightarrow \pi^*$ and $\pi^* \rightarrow \pi^*$ transitions, are present as principal features in the spectrum of Li(bipy)[28] and are reasonably ascribed to radical anion signatures in this ytterbocene adduct. If correct, the absorption coefficients are low, implying a low concentration of 3,3′-Me_2bipy radical anion. The intensity of the ligand-based $\pi^* \rightarrow \pi^*$ transitions and the relatively small spread of the ^{1}H NMR chemical shifts imply that the extent of the paramagnetism of $Cp^*_2Yb(3,3'$-

dx.doi.org/10.1021/om400528d | Organometallics XXXX, XXX, XXX−XXX

Table 2. Comparison of Bond Lengths (Å) and Angles (deg) for $Cp^*_2Yb(3,3'\text{-}Me_2bipy)$ and $[Cp^*_2Yb(3,3'\text{-}Me_2bipy)]^+$

	$Cp^*_2Yb(3,3'\text{-}Me_2bipy)$	$[Cp^*_2Yb(3,3'\text{-}Me_2bipy)]^+$	Δ^a
Yb−C(ring) (av)	2.71 ± 0.01	2.60 ± 0.01	0.11
Yb−C(ring) (range)	2.693(3)−2.732(3)	2.585(4)−2.629(4)	
Yb−Cp(cent)	2.43	2.31	0.12
Yb−N (av)	2.485 ± 0.003	2.393 ± 0.002	0.09
C(25)−C(26)	1.494(5)	1.491(6)	0.003
Cp(cent)−Yb−Cp(cent)	147	141	6
Cp(cent)−Yb−N	103, 107	105, 108	2, 1
N−Yb−N	66.6(1)	69.6(1)	−3
N−C−C−N	38	37	1
C−C−C−C	44	43	1
3-Me-2-pyridyl	41	41	0

[a] Δ is the value in the neutral adduct minus that in the cation in Å or deg.

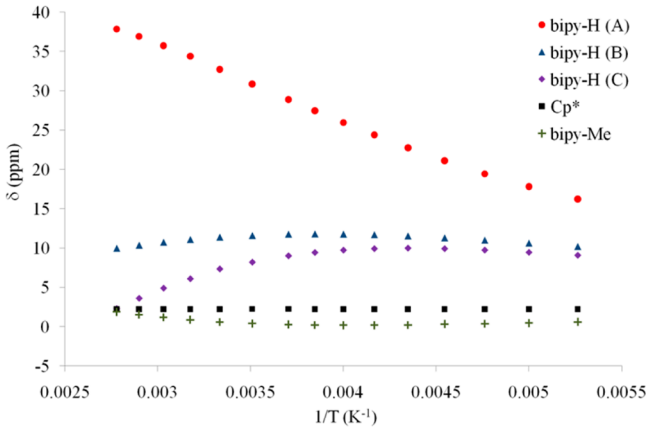

Figure 3. Chemical shift (δ) vs $1/T$ plot of the proton resonances of $Cp^*_2Yb(3,3'\text{-}Me_2bipy)$ in toluene-d_8 over a temperature range of 180 to 360 K.

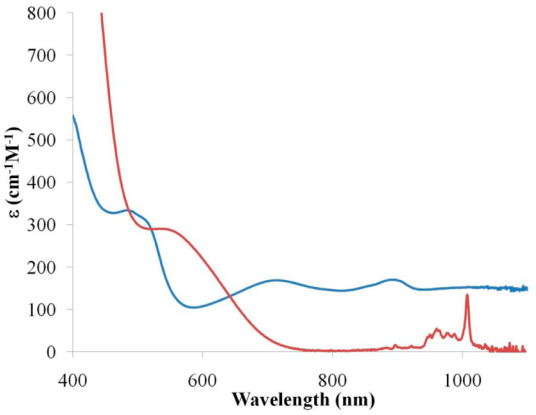

Figure 4. Room-temperature visible spectra of $Cp^*_2Yb(3,3'\text{-}Me_2bipy)$ (blue line) in toluene and $[Cp^*_2Yb(3,3'\text{-}Me_2bipy)][Cp^*_2YbCl_{1.5}I_{0.5}]$ (red line) in CH_2Cl_2.

Me_2bipy) is small, which in turns implies that the f^{14} configuration dominates the $f^{13}(bipy^{\bullet-})$ configuration in the ground state electronic structure.

The cation in $[Cp^*_2Yb(3,3'\text{-}Me_2bipy)][Cp^*_2YbCl_{1.5}I_{0.5}]$ possesses a simpler visible spectrum at room temperature and is similar to the reported spectra of cationic Cp^*_2Yb adducts with N-aromatic heterocycles.[11,28] The presence of several f−f transitions in the 950−1020 nm range accounts for the multiple coordination environments of the anionic partner in the anion pair.

Magnetism and XANES Studies. The effective magnetic moment at 300 K for $Cp^*_2Yb(3,3'\text{-}Me_2bipy)$ is 0.8 μ_B, low relative to the value expected for two uncorrelated spin carriers, Yb(III) f^{13} and $bipy^{\bullet-}$, for which a value of 4.85 μ_B is expected. The low value of μ_{eff} is an indication that the Yb in the neutral adduct may be intermediate valent and therefore a member of the family of the bipyridine adducts of Cp^*_2Yb reported earlier in which effective moments range from 2.4 to 0.8 μ_B at 300 K. The temperature dependence of μ_{eff} from 2 to 300 K is shown in Figure 5 (plots of χ, $1/\chi$, and χT vs T are available in the Supporting Information).

The value of μ_{eff} decreases slowly in the neutral adduct with decreasing temperature to a value of 0.6 μ_B at 30 K and then rapidly decreases to 0.3 μ_B at 2 K. The latter decrease is likely due to intermolecular antiferromagnetic coupling at low temperature, as previously observed.[1] In contrast, and as expected, the value of μ_{eff} for $[Cp^*_2Yb(3,3'\text{-}Me_2bipy)]$-$[Cp^*_2YbI_2]$ of 6.1 μ_B is in accord with the value for two Yb(III) $^2J_{7/2}$ isolated paramagnets of 6.4 μ_B. Although the low effective moment for the neutral adduct is a signature of intermediate-valent ytterbium, a spectroscopic measurement is necessary to confirm this hypothesis. The Yb L_{III}-edge XANES[1,3] spectra in Figure 6 show that the measurements at 30 and 300 K are nearly superimposable and therefore the ratio of Yb(II) f^{14} to Yb(III) f^{13} is independent of temperature; this rules out a valence tautomeric equilibrium as a possible explanation for the temperature dependence of μ_{eff}. The XANES spectra can be fit into f^{14} and f^{13} components in a ratio of 83:17 at both temperatures, and the resulting n_f value is therefore 0.17. These results place $Cp^*_2Yb(3,3'\text{-}Me_2bipy)$ into a small subset of bipyridine adducts with low values of μ_{eff} and n_f at 300 K reported previously (Table 3).

In the first two adducts in Table 3, the metallocenes are bipy adducts of $(C_5Me_5)_2Yb$ in which the substituents on the bipyridines are methyl groups in the 3,3′-positions and methoxy groups in the 4,4′-positions. These two groups are electron donating, since the reduction potentials of the corresponding free ligands are more negative than that in unsubstituted bipy and therefore more difficult to reduce (Table 1). The third and fourth adducts given in Table 3 show the influence of the substituents on the metallocene: C_5Me_5 is more strongly reducing than C_5H_4Me, as shown in Table 1, and presumably C_5H_5, consistent with the relative value of n_f; therefore, the intermediate valence of ytterbium can be influenced by the redox potentials of the individual fragments

dx.doi.org/10.1021/om400528d | Organometallics XXXX, XXX, XXX−XXX

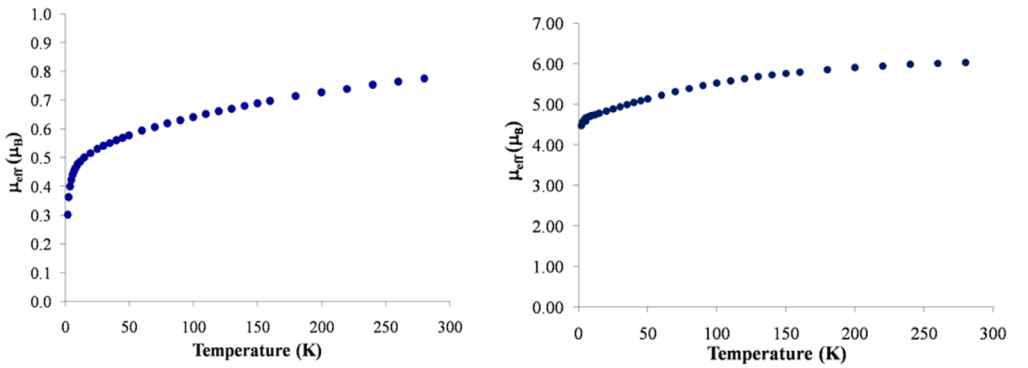

Figure 5. Temperature-dependent magnetic susceptibility data for the neutral (left) and cationic ytterbocenes (right) between 2 and 300 K.

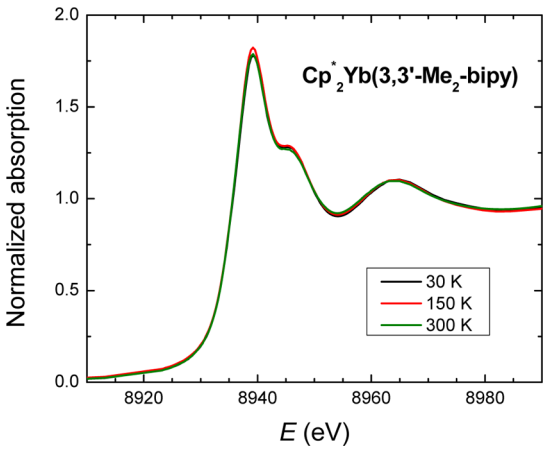

Figure 6. Yb L_{III}-edge XANES spectra for $Cp^*_2Yb(3,3'\text{-}Me_2bipy)$ at 30, 150, and 300 K. The main peak at 8939 eV is indicative of the Yb(II) contribution, and the peak at 8946 eV is indicative of the Yb(III) contribution.

Table 3. μ_{eff} and n_f Values for Some Selected $Cp_2'Yb(x,x'\text{-bipy})$ Adducts

Cp′	x,x′	μ_{eff} (μ_B)	n_f(300 K)	ref
C_5Me_5	3,3′-Me_2	0.8	0.17(2)	this work
C_5Me_5	4,4′-$(OMe)_2$	1.1	0.13(9)	1, 12
C_5H_5	H,H	1.2	0.30(1)	1, 22
C_5Me_5	H,H	2.4	0.83(2)	1
C_5Me_5	4,4′-CO_2Me	3.2	0.84(2)	1

in the adducts. This element of control was advanced in earlier work,[1,3] and the new adduct described here provides additional support for and extends this postulate to a geometrical dependence of the bipyridine ligands.

Calculations. The CASSCF methodology, similar to methods used in previous studies, gives the calculated singlet−triplet energy separations and n_f values shown in Table 4.

Table 4. CASSCF Calculational Results

	S−T gap (eV)	n_f(calcd)	n_f(exptl)
$(C_5H_5)_2Yb(bipy)$	−0.6	0.32	0.30
$(C_5Me_5)_2Yb(bipy)$	−0.28[3]	0.86[3]	0.83[1]
$(C_5Me_5)_2Yb(3,3'\text{-}Me_2bipy)$	−0.28	0.27	0.17
$(C_5Me_5)_2Yb(4,4'\text{-}(MeO)_2bipy)$	−0.007	0.11	0.13

The calculational results are consistent with those obtained on related bipy adducts, in that the electronic ground states are open-shell singlet states that are multiconfigurational. Only one singlet is found below the triplet in each adduct in Table 4. The singlet state is composed of the two configurations $f^{13}(\pi_1^*)^1$ and $f^{14}(\pi_1^*)^0$; the $f^{12}(\pi_1^*)^2$ configuration is less than 2%. The calculated values of n_f agree with the experimental values very well for $(C_5H_5)_2Yb(bipy)$ and $(C_5Me_5)_2Yb(4,4'\text{-}(OMe)_2bipy)$, but the agreement is less good for the 3,3′-Me_2bipy adduct. In each case, the dominant configuration is f^{14}, in contrast to the results for $(C_5Me_5)_2Yb(bipy)$.

DISCUSSION

The original reason for preparing the 3,3′-Me_2bipy adduct of Cp^*_2Yb was to determine the role of the torsion angle of the bipyridine ligand on the intermediate valence of ytterbium in the resulting adduct. The NCCN torsion angle in the x,x′-Me_2bipy adducts of Cp^*_2Yb are small; the torsion angles are 1 and 4° for 4,4′-Me_2bipy and 5,5′-Me_2bipy adducts, respectively, and the 2-pyridyl rings are nearly coplanar.[3,12] When the methyl groups are in the 3,3′-positions of the 2-pyridyl rings, the rings are forced out of planarity. The twisted geometry raises the energy of the LUMO, π_1^*, and the reduction potential of the free ligand (see Table 1), which in turn affects the configuration of the open-shell singlet ground state and ultimately the magnetism of the adduct. This expectation is met in $Cp^*_2Yb(3,3'\text{-}Me_2bipy)$ since the torsion angle is 38°; the magnetic moment is one of the lowest observed at 300 K, as is the n_f value of 0.17. These experimental results are in reasonable agreement with the calculated value of n_f in Table 4, and the dominant configuration of the open-shell singlet ground state is $f^{14}(\pi_1^*)$.

The connection between n_f and the redox properties of the ytterbocene and the bipyridine ligand can be extended to $Cp^*_2Yb(4,4'\text{-}(MeO)_2bipy)$ and $Cp_2Yb(bipy)$, two adducts with low values of n_f are 0.13 and 0.30, respectively, which are independent of temperature. A methoxy group is a better electron donor than a methyl group; the Hammett σ_p values are −0.27 and −0.17, respectively,[29] and the reduction potential of 4,4′-$(EtO)_2$-bipy is 0.20 V more negative than that of 4,4′-Me_2bipy (Table 1). The n_f value for $Cp^*_2Yb(4,4'\text{-}(MeO)_2bipy)$ is 0.13, in accord with the larger reduction potential of the free ligand. The calculated value of n_f of 0.11 agrees with the experimental value. The reduction potential of $(C_5Me_5)_2Yb^+$ is more negative than that of $(C_5H_4Me)_2Yb^+$ by 0.13 V (Table 1); the value for $(C_5H_5)_2Yb^+$ is not available but is likely to be slightly lower. The n_f values of the adducts of $(C_5Me_5)_2Yb$ and

dx.doi.org/10.1021/om400528d | Organometallics XXXX, XXX, XXX−XXX

$(C_5H_5)_2Yb$ with bipy are 0.83 and 0.30, respectively, consistent with the proposition advanced above. The calculated values of n_f of 0.86 and 0.32 agree with experiment, and these values show that the dominant configuration in the multiconfigurational ground state is inverted by changing the number of methyl substituents on the cyclopentadienyl rings.

The relation between the redox potential and n_f provides a guide to the extent of unpaired spin density located in the bipy and related heterocyclic amine adducts of ytterbocenes. The redox properties of the uncoordinated fragments in the molecular adducts, however, are only a guide, since these values change on coordination; the redox potentials in Table 1 show that Cp^*_2Yb is thermodynamically incapable of reducing bipy, but electron transfer does occur. The distribution of unpaired spin density in the ligand orbitals, after the initial electron transfer event, alters the configurations involved in the multiconfigurational ground state and therefore the magnetic properties of the adducts. The amount of unpaired spin density at a given site in the ligand orbitals is crucial for understanding chemical reactivity, which is our ultimate goal. One such example, cleavage of a specific C−H bond in the 4,5-diazafluorene adduct of Cp^*_2Yb, has been reported[30] and the other will be reported in due course.

CONCLUSIONS

The experimental and computational studies outlined in this and previous articles[1,3] on the adducts formed between various ytterbocenes and substituted bipyridine ligands develops a model that accounts for their unusual magnetic properties. The experimental facts are that the ytterbium adducts are intermediate-valent molecular compounds; that is, the valence of ytterbium is neither Yb(II), f^{14}, nor Yb(III), f^{13}, but lies between these two extreme values. The electronic ground state is comprised of two configurations, $f^{14}(\pi_1^*)^0$ and $f^{13}(\pi_1^*)^1$, resulting in an open-shell singlet ground state that lies below the triplet state. The relative population of these two configurations, expressed as n_f, depends on the redox properties of the individual fragments of the adducts. Accordingly, the substituents on each fragment play a role in determining the composition of the multiconfigurational ground state and ultimately the magnetic properties of the resulting adducts.[31] The multiconfigurational ground state is, in this model, the way ytterbium avoids the extreme values of its possible oxidation numbers, which allows the adducts to obey Pauling's electroneutrality principle and behave as if they are covalent molecules.[31−33]

EXPERIMENTAL SECTION

General Considerations. All reactions were performed using standard Schlenk-line techniques or in a drybox (MBraun). All glassware was dried at 150 °C for at least 12 h prior to use. Toluene and pentane were dried over sodium and distilled, while CH_2Cl_2 was purified by passage through a column of activated alumina. Toluene-d_8 and C_6D_6 were dried over sodium. All the solvents were degassed prior to use. Infrared samples were prepared as Nujol mulls and taken between KBr plates and recorded on a Thermo Scientific Nicolet IS10 spectrometer. Samples for ultraviolet, visible, and near-infrared spectrometry were prepared in a Schlenk-adapted quartz cuvette, and spectra were obtained using a Varian Cary 50 scanning spectrophotometer. Melting points were determined in sealed capillaries prepared under nitrogen and are uncorrected. Elemental analyses and mass spectra (EI) were determined by the Microanalytical Laboratory of the College of Chemistry, University of California, Berkeley. X-ray structural determinations were performed at CHEXRAY, University of California, Berkeley. Magnetic susceptibility measurements were made for all samples at 5 and 40 kOe in a 7 T Quantum Design Magnetic Properties Measurement System, which utilizes a superconducting quantum interference device (SQUID). Sample containment and other experimental details have been described previously.[22] The samples were prepared for X-ray absorption experiments as described previously, and the same methods were used to protect the air-sensitive compounds from oxygen and water.[1] X-ray absorption measurements were made at the Stanford Synchrotron Radiation Lightsource on beamline 11-2. The samples were prepared and loaded into a liquid helium-flow cryostat at the beamline, as described previously.[1] Data were collected at temperatures ranging from 30 to 300 K, using a Si(220) double-crystal monochromator. Fit methods were the same as those described previously.[1]

Table 5. Selected Crystal Data for $Cp^*_2Yb(3,3'\text{-}Me_2bipy)$ and $[(Cp^*_2Yb(3,3'\text{-}Me_2bipy)][Cp^*_2YbCl_{1.6}I_{0.4}]\cdot CH_2Cl_2$

	$Cp^*_2Yb(3,3'\text{-}Me_2bipy)$	$[(Cp^*_2Yb(3,3'\text{-}Me_2bipy)][Cp^*_2YbCl_{1.6}I_{0.4}]\cdot CH_2Cl_2$
formula	$C_{32}H_{42}N_2Yb$	$C_{53}H_{74}N_2Cl_{3.6}I_{0.4}Yb_2$
cryst size (mm)	0.3 × 0.25 × 0.10	0.45 × 0.37 × 0.15
cryst syst	orthorhombic	triclinic
space group	*Pbca*	$P\bar{1}$
V (Å^3)	5827(3)	2582.8(6)
a (Å)	17.550(5)	9.4957(14)
b (Å)	18.129(5)	17.024(2)
c (Å)	18.314(5)	17.198(3)
α (deg)	90	72.940(2)
β (deg)	90	76.451(2)
γ (deg)	90	87.439(2)
Z	8	2
formula wt	627.72	1263.65
calcd density (g cm^{-3})	1.431	1.749
abs coeff (mm^{-1})	3.247	4.060
F(000)	3024	1322
temp (K)	153(2)	110(2)
diffractometer	SMART APEX	SMART 1000
θ range for data collection (deg)	1.96−25.34	2.44−25.48
transmission range	0.393−0.723	0.132−0.481
abs cor	multiscan	multiscan
total no. of rflns	49048	41199
no. of unique rflns (R_{int})	5319 (0.0455)	9410 (0.0264)
final R indices ($I > 2\sigma(I)$)	R = 0.0247, R_w = 0.0522	R = 0.0280, R_w = 0.0684
R indices (all data)	R = 0.0354, R_w = 0.0574	R = 0.0328, R_w = 0.0706
largest diff peak and hole (e Å^{-3})	1.518 and −0.732	1.521 and −0.901
GOF	1.078	1.047

Calculations. The ytterbium center was treated with a small-core relativistic pseudopotential (RECP) ([Ar] + 3d)[34] in combination with its adapted basis set (a segmented basis set that includes up to g functions). The carbon, nitrogen, oxygen, and hydrogen atoms were treated with an all-electron double-ζ, 6-31G(d,p),[35] basis set. All the calculations were carried out with the Gaussian 03 suite of programs[36] and ORCA suite of program[37] either at the density functional theory (DFT) level using the B3PW91[38] hybrid functional or at the CASSCF level; only one active space and inactive orbitals were used in the calculation. The geometry optimizations were performed without any symmetry constraints at either the DFT or the CASSCF level. The electrons were distributed over four 4f orbitals and the two π^* orbitals in the bipyridines. The CASSCF calculations were done using the SCF orbitals. The subsequent analysis of the mixture of configuration was achieved by projecting the wave function on the initial orbitals, namely

dx.doi.org/10.1021/om400528d | Organometallics XXXX, XXX, XXX−XXX

the SCF orbitals. This ensures that no mixing between f and π^* is present in the starting set of orbitals.

Ligand. The original synthesis of 3,3′-dimethyl-2,2′-bipyridine (3,3′-Me_2bipy) described in the literature used the Ullmann methodology to couple two 2-bromo-3-methylpyridine molecules.[39] The bipyridine was reported as a viscous liquid with bp 293−298 °C (1 atm). A slight modification was later reported,[40] and the ligand was described as a colorless liquid whose UV spectrum agreed with the literature values.[41] A ^{1}H NMR spectrum in Me_2CO-d_6 was reported somewhat later.[42] The ligand used in the work reported here was purchased from SYNTHON Chemical (ChemiePark Bitterfeld Wolfen Area A, Werkstattstrasse 10, 06 766 Wolfen, Germany) as a white crystalline solid that sublimed at 90−100 °C onto a water-cooled cold finger under dynamic vacuum (~10^{-2} mm). ^{1}H NMR (C_6D_6, 293 K, δ (ppm)): 8.45 (d, $J_{5,6}$ = 4 Hz, 2H, 6-H), 7.08 (d, $J_{4,5}$ = 8 Hz, 2H, 4-H), 6.71 (dd, $J_{4,5}$ = 8.5 Hz, $J_{5,6}$ = 5 Hz, 2H, 5-H), 2.12 (s, 6H, Me). The ultimate proof that pure 3,3′-Me_2bipy is a solid was obtained from the X-ray crystal structures of the adducts described below.

Cp*$_2$Yb(3,3′-Me$_2$bipy). The complex Cp*$_2$Yb(OEt$_2$) (0.325 g, 0.629 mmol) was combined with 3,3′-dimethyl-2,2′-bipyridine (3,3′-Me_2bipy, 0.116 g, 0.629 mmol), and toluene (50 mL) was added at room temperature. The brown suspension was stirred at room temperature for 2 h, concentrated to ca. 25 mL, and cooled to −20 °C. A dark green microcrystalline powder formed overnight (323 mg, 82%), which was recrystallized at −20 °C from warm toluene (40 °C). X-ray -suitable dark green crystals formed (160 mg, 41%). The filtrate was concentrated to 15 mL and cooled to −20 °C. Second and third crops of crystals were obtained (77 mg, combined yield 70%). ^{1}H NMR (toluene-d_8, 300 K, δ (ppm)): 32.71 (2H), 12.12 (2H, d, J = 6 Hz), 8.49 (2H), 2.23 (30H, Me_5C_5), 0.58 (6H, Me). Mp: 310−313 °C. Anal. Calcd for $C_{32}H_{42}N_2Yb$: C, 61.23; H, 6.74; N, 4.46. Found: C, 61,45; H, 6.47; N, 4.32. IR (cm^{-1}): 1567 (m), 1436 (s), 1411 (m), 1380 (w), 1090 (w), 1064 (w), 1040 (w), 790 (m), 741 (m), 698 (w).

[Cp*$_2$Yb(3,3′-Me$_2$bipy)]$^+$[Cp*$_2$YbI$_2$]$^-$. The complex Cp*$_2$Yb(OEt$_2$) (0.204 g, 0.394 mmol) was combined in the drybox with 3,3′-Me_2bipy (0.073g, 0.394 mmol) and AgI (0.093g, 0.394 mmol). Toluene (20 mL) was added at room temperature, and the brown suspension was stirred at room temperature for 16 h (overnight). The resulting brown suspension was filtered, and the solvent was removed under reduced pressure. The solid was triturated in pentane, the pentane was removed under reduced pressure, and the residue was crystallized from warm toluene. The crystals were recrystallized twice from warm toluene (185 mg, 36%). Toluene in the ratio 1:0.33 was found in the ^{1}H NMR spectrum and by elemental analysis. ^{1}H NMR (CD_2Cl_2, 300 K, δ (ppm)): 331.3 (2H), 58.51 (2H), 9.84 (2H), 7.28−7.17 (m, 1.7 H, toluene), 4.17 (30H, Me_5C_5), 3.78 (30H, C_5Me_5), 2.10 (s, 1H, toluene), −17.81 (6H, Me). ^{1}H NMR (toluene-d_8, 300 K, δ (ppm)): 58.46 (2H), 10.38 (2H), 6.98 (30H, Me_5C_5), 4.31 (30H, C_5Me_5), −17.59 (6H, Me). The downfield resonance due to 2H was not found in toluene. Mp: >330 °C. Anal. Calcd for $C_{54.33}H_{74.67}N_2I_2Yb_2$ (**2**·0.33Tol): C, 48.13; H, 5.55; N, 2.07. Found: C, 48.17; H, 5.36; N, 2.14. IR (cm^{-1}): 1604 (m), 1580 (m), 1437 (s), 1378 (m), 1188 (w), 1130 (w), 1113 (w), 1027 (w), 794 (w), 720 (m), 695 (w).

[Cp*$_2$Yb(3,3′-Me$_2$bipy)][Cp*$_2$YbCl$_{1.6}$I$_{0.4}$]·CH$_2$Cl$_2$. When the product of the reaction was recrystallized by layering pentane on top of CH_2Cl_2, instead of toluene, crystals suitable for an X-ray determination were obtained in better yield (75%); however, some of the iodide atoms were replaced by chlorine atoms. In the X-ray experiment, the compound was found to cocrystallize with CH_2Cl_2, giving the empirical formula [(Cp*$_2$Yb(3,3′-Me_2bipy)]-[Cp*$_2$YbCl$_{1.6}$I$_{0.4}$]·CH_2Cl_2. The combustion analysis fits a slightly different formula: [(Cp*$_2$Yb(3,3′-Me_2bipy)][Cp*$_2$YbCl$_{1.5}$I$_{0.5}$]·CH_2Cl_2. Anal. Calcd for $C_{53}H_{74}N_2I_{0.5}Cl_{3.5}Yb_2$: C, 50.01; H, 5.86; N, 2.20. Found: C, 49.72; H, 5.52; N, 2.26. IR (cm^{-1}): 2850 (s), 2713 (w), 1582 (m), 1573 (m), 1439 (s), 1406 (m), 1378 (s), 1280 (m), 1237 (w), 1191(w), 1182 (w), 1167 (w), 1019 (s), 992 (w), 851 (m), 796 (s), 731 (s), 708 (m), 700 (m), 616 (w), 593 (w).

X-ray Crystallography. Single crystals of the compounds Cp*$_2$Yb(3,3′-Me_2bipy) and [(Cp*$_2$Yb(3,3′-Me_2bipy)]-[Cp*$_2$YbCl$_{1.6}$I$_{0.4}$]·CH_2Cl_2 were coated in Paratone-N oil and mounted on a Kaptan loop. The loop was transferred to Bruker SMART 1000[43] and SMART APEX diffractometers equipped with a CCD area detector for Cp*$_2$Yb(3,3′-Me_2bipy) and [(Cp*$_2$Yb(3,3′-Me_2bipy)]-[Cp*$_2$YbCl$_{1.6}$I$_{0.4}$]·CH_2Cl_2, respectively,[44] Preliminary orientation matrices and cell constants were determined by collection of 10 s frames, followed by spot integration and least-squares refinement. Data were intergrated by the program SAINT[45] to a maximum 2θ value of 50.68° for Cp*$_2$Yb(3,3′-Me_2bipy) and 50.96° for [(Cp*$_2$Yb(3,3′-Me_2bipy)][Cp*$_2$YbCl$_{1.6}$I$_{0.4}$]·CH_2Cl_2. The data were corrected for Lorentz and polarization effects. Data were analyzed for agreement and possible absorption using XPREP. A semiempirical multiscan absorption correction was applied using SADABS.[46] This models the absorption surface using a spherical harmonic series based on differences between equivalent reflections. The structures were solved by direct methods using SHELX[47] and the WinGX program.[48] Non-hydrogen atoms were refined anisotropically, and hydrogen atoms were placed in calculated positions and not refined. Selected crystal data are given in Table 5.

■ ASSOCIATED CONTENT

Supporting Information

Text, tables, figures, and CIF files giving information concerning magnetic susceptibility, vis−near-IR spectroscopy, ^{1}H variable-temperature NMR, X-ray crystal data for Cp*$_2$Yb(3,3′-Me_2bipy) (CCDC 943122) and [Cp*$_2$Yb(3,3′-Me_2bipy)][Cp*$_2$YbCl$_{1.6}$I$_{0.4}$]·CH_2Cl_2 (CCDC 943123), and calculated Cartesian coordinates for Cp_2Yb(bipy), Cp*$_2$Yb(3,3′-Me_2bipy), and Cp*$_2$Yb(4,4′-$(OMe)_2$bipy). This material is available free of charge via the Internet at http://pubs.acs.org.

■ AUTHOR INFORMATION

Corresponding Authors

*E-mail for G.N.: greg.nocton@polytechnique.edu.
*E-mail for R.A.A.: raandersen@lbl.gov.

Notes

The authors declare no competing financial interest.

■ ACKNOWLEDGMENTS

Work at the University of California, Berkeley, and at Lawrence Berkeley National Laboratory was supported by the Director, Office of Energy Research, Office of Basic Energy Sciences, Chemical Sciences Division, of the U.S. Department of Energy under Contract No. DE-AC02-05CH11231. X-ray absorption data were collected at the Stanford Synchrotron Radiation Lightsource, a Directorate of SLAC National Accelerator Laboratory and an Office of Science User Facility operated for the U.S. Department of Energy Office of Science by Stanford University. We thank Wayne Lukens for several discussions on the Hubbard molecular model and Antonio DiPasquale at CHEXRAY Berkeley for his help with crystal structures.

■ REFERENCES

(1) Booth, C. H.; Walter, M. D.; Kazhdan, D.; Hu, Y.-J.; Lukens, W. W.; Bauer, E. D.; Maron, L.; Eisenstein, O.; Andersen, R. A. *J. Am. Chem. Soc.* **2009**, *131*, 6480.

(2) Neumann, C. S.; Fulde, P. *Z. Phys. B: Condens. Matter* **1989**, *74*, 277.

(3) Booth, C. H.; Kazhdan, D.; Werkema, E. L.; Walter, M. D.; Lukens, W. W.; Bauer, E. D.; Hu, Y.-J.; Maron, L.; Eisenstein, O.; Head-Gordon, M.; Andersen, R. A. *J. Am. Chem. Soc.* **2010**, *132*, 17537.

(4) Bordon, W. T. *Effects of Electron Repulsion in Diradicals*; New York, 1982.

(5) Tabner, B. J.; Yandle, J. R. *J. Chem. Soc. A* **1968**, 381.
(6) McInnes, E. J. L.; Farley, R. D.; Rowlands, C. C.; Welch, A. J.; Rovatti, L.; Yellowlees, L. J. *J. Chem. Soc., Dalton Trans.* **1999**, 4203.
(7) Klein, A.; Kaim, W.; Waldhor, E.; Hausen, H. D. *J. Chem. Soc., Perkin Trans. 2* **1995**, 2121.
(8) Finke, R. G.; Keenan, S. R.; Schiraldi, D. A.; Watson, P. L. *Organometallics* **1986**, *5*, 598.
(9) Watson, P. L.; Tulip, T. H.; Williams, I. *Organometallics* **1990**, *9*, 1999.
(10) Tilley, T. D.; Boncella, J. M.; Berg, D. J.; Burns, C. J.; Andersen, R. A. *Inorg. Synth.* **1990**, *27*, 146.
(11) Schultz, M.; Boncella, J. M.; Berg, D. J.; Tilley, T. D.; Andersen, R. A. *Organometallics* **2002**, *21*, 460.
(12) Walter, M. D.; Berg, D. J.; Andersen, R. A. *Organometallics* **2006**, *25*, 3228.
(13) Tilley, T. D.; Andersen, R. A.; Spencer, B.; Zalkin, A. *Inorg. Chem.* **1982**, *21*, 2647.
(14) Ohba, S.; Sato, S.; Saito, Y. *Acta Crystallogr., Sect. B* **1979**, *35*, 957.
(15) Ohba, S.; Miyamae, H.; Sato, S.; Saito, Y. *Acta Crystallogr., Sect. B* **1979**, *35*, 1470.
(16) Baxter, P. N. W.; Connor, J. A.; Wallis, J. D.; Povey, D. C.; Powell, A. K. *Polyhedron* **1992**, *11*, 1771.
(17) Cheng, W.-C.; Yu, W.-Y.; Zhu, J.; Cheung, K.-K.; Peng, S.-M.; Poon, C.-K.; Che, C.-M. *Inorg. Chim. Acta* **1996**, *242*, 105.
(18) Craig, D.; Goodwin, H.; Onggo, D. *Aust. J. Chem.* **1988**, *41*, 1157.
(19) Varela, J. A.; Castedo, L.; Maestro, M.; Mahía, J.; Saá, C. *Chem. Eur. J.* **2001**, *7*, 5203.
(20) Sato, S.; Saito, Y. *Acta Crystallogr., Sect. B* **1978**, *34*, 3352.
(21) The H-3 and H-5 resonances in ref 12 are incorrectly assigned; the correct assignment is in ref 3.
(22) Walter, M. D.; Schultz, M.; Andersen, R. A. *New J. Chem.* **2006**, *30*, 238.
(23) Banci, L.; Bertini, I.; Luchinat, C.; Pierattelli, R.; Shokhirev, N. V.; Walker, F. A. *J. Am. Chem. Soc.* **1998**, *120*, 8472.
(24) Oki, M. *Top. Stereochem.* **1983**, *14*, 1.
(25) Ashby, M. T.; Alguindigue, S. S.; Schwane, J. D.; Daniel, T. A. *Inorg. Chem.* **2001**, *40*, 6643.
(26) Ashby, M. T. *J. Am. Chem. Soc.* **1995**, *117*, 2000.
(27) Ashby, M. T.; Alguindigue, S. S.; Khan, M. A. *Organometallics* **2000**, *19*, 547.
(28) Da Re, R. E.; Kuehl, C. J.; Brown, M. G.; Rocha, R. C.; Bauer, E. D.; John, K. D.; Morris, D. E.; Shreve, A. P.; Sarrao, J. L. *Inorg. Chem.* **2003**, *42*, 5551.
(29) Streitweiser, A.; Heathcock, C. H.; Kosower, E. M. *Introduction to Organic Chemistry*; Macmillan: New York, 1992.
(30) Nocton, G.; Booth, C. H.; Maron, L.; Andersen, R. A. *Organometallics* **2013**, *32*, 1150.
(31) Lukens, W. W.; Magnani, N.; Booth, C. H. *Inorg. Chem.* **2012**, *51*, 10105.
(32) Denning, R. G.; Harmer, J.; Green, J. C.; Irwin, M. *J. Am. Chem. Soc.* **2011**, *133*, 20644.
(33) Neidig, M. L.; Clark, D. L.; Martin, R. L. *Coord. Chem. Rev.* **2013**, *257*, 394.
(34) Dolg, M.; Stoll, H.; Preuss, H. *J. Chem. Phys.* **1989**, *90*, 1730.
(35) Harihara, Pc; Pople, J. A. *Theor. Chim. Acta* **1973**, *28*, 213.
(36) Frisch, J., et al. *Gaussian 03, Revision E-01 ed.*; Gaussian Inc., Pittsburgh, PA, 2001.
(37) Neese, F. *ORCA, Version 2.4 ed.*; Chemie, M.-P.-I. f. B., Ed. Mülheim an der Ruhr, 2004.
(38) Becke, A. D. *J. Chem. Phys.* **1993**, *98*, 5648.
(39) Case, F. H. *J. Am. Chem. Soc.* **1946**, *68*, 2574.
(40) Nakamaru, K. *Bull. Chem. Soc. Jpn.* **1982**, *55*, 2697.
(41) Suzuki, T. M.; Kimura, T. *Bull. Chem. Soc. Jpn.* **1977**, *50*, 391.
(42) Rebek, J.; Trend, J. E.; Wattley, R. V.; Chakravorti, S. *J. Am. Chem. Soc.* **1979**, *101*, 4333.
(43) Bruker Analytical X-Ray Systems, Madison, WI, 2007.
(44) Bruker Analytical X-Ray Systems, Madison, WI, 2007.
(45) Bruker Analytical X-Ray Systems, Madison, WI, 2007.
(46) Blessing, R. *Acta Crystallogr., Sect. A* **1995**, *51*, 33.
(47) Sheldrick, G. *Acta Crystallogr., Sect. A* **2008**, *64*, 112.
(48) Farrugia, L. *J. Appl. Crystallogr.* **1999**, *32*, 837.